Dye-sensitized solar cells on TiO_2 Photoelectrodes sensitized with rhodamine

Bandana Ranamagar, Isaac Abiye, Fasil Abebe*

Department of Chemistry, Morgan State University, Baltimore, MD, 21251

*Author to whom correspondence should be addressed; E-mail: Fasil.Abebe@morgan.edu

ABSTRACT

Rhodamine-6G derivative **Rhd**, synthesized by microwave-assisted condensation of rhodamine hydrazide and 2-Amino-3-formylchromone, and its metal complexes were investigated using ultraviolet-visible (UV-Vis) and fluorescence spectroscopy. Dye-sensitized solar cells (DSSCs) were fabricated using **Rhd** and its metal complexes with aluminum (Al^{3+}) and chromium ions (Cr^{3+}). Current-density (I-V) characteristics and Electrochemical Impedance Spectroscopy (EIS) measurements of the rhodamine dyes were conducted to determine their solar-to-electric power efficiencies and electron lifetimes. The solar cell sensitized with **Rhd** and Cr^{3+} had the highest solar to electric power efficiency at 0.16%.

Key words: Optical, Cations, Dye-sensitized solar cell, TiO_2, Rhodamine

1. Introduction

The creation of an accessible, non-depletable, renewable, and clean solar energy technology has been the subject of research from the very beginning for longer-term gains. Both from a scientific/academic and an industrial standpoint, biomass, biofuel, hydropower, geothermal energy, solar energy, and wind power have all been thoroughly investigated. However, solar energy is now thought to be the most promising renewable resource [1-2]. In 1991, Michael Gratzel and a colleague invented dye-sensitized solar cells (DSSCs), which are inexpensive and simple to make into photovoltaic systems. The number of studies focused on the large-scale production of DSSCs, and their optimization has grown exponentially. A photosensitizing dye is used in DSSCs to convert solar energy into electrical energy. The three fundamental steps in producing electricity in DSSCs are charge separation, solar energy collection, and catalytic reactions [3-4]. DSSCs are

made up of just five elements: a counter electrode, a transparent conductive oxide (FTO) substrate, a visible-light absorber dye (Rhodamine-6G), a nanostructured n-type semiconductor (TiO_2), and an electrolyte (I^-/I_3^-) [5]. Distinct types of dye have been used to fabricate DSSCs with varying solar-to-electricity conversion efficiencies, and some among them are rhodamine dyes [6].

Rhodamine is a reasonably priced broad band photosensitizer with good visible and near-infrared absorption spectra, and it has the essential characteristics needed to function as a photosensitizer. The current work describes an investigation of the DSSC characteristics of rhodamine dye based on (TiO_2) electrodes [7]. The long absorption and emission wavelengths, high fluorescence quantum yield, high extinction coefficient, and outstanding photostability of rhodamine dyes also make Rhodamine ideal for use in fluorescent sensor fabrication [8-9].

2. Experimental

2.1 Materials and methods

All the reagents and solvents were acquired from Sigma-Aldrich including Rhodamine-6G, hydrazine hydrate (85%), 2-Amino-3-formylchromone, ethanol, acetic acid, and salts. The titanium dioxide (TiO_2) film was prepared with Titanium (IV) oxide, anatase powder purchased from Sigma-Aldrich. Water-based colloidal graphite used in making the counter electrode was purchased from Electron Microscopy Sciences (EMS). The conducting fluorine-doped tin oxide (FTO) glass substrate was obtained from Sigma-Aldrich.

The performance of the solar cell was evaluated using a 150 W fully reflective SciSun-150 solar simulator with air-mass 1.5 global (AM 1.5 G) illumination, which comes with an irradiance of 100 mW/cm^2 (Sciencetech Inc.) (London, Ontario, Canada), and the Interface 1010E potentiostat/galvanostat/ZRA was purchased from GAMRY Instruments (Warminster, PA). All absorption and fluorescence spectra were recorded using Agilent Cary 60 UV/Vis's and Cary Eclipse fluorescence spectrophotometer, respectively.

2.2 Fabrication of the Dye-Sensitized Solar Cell

The titanium dioxide paste was prepared by mixing TiO_2 powder, ethylene glycol, and glacial acetic acid [13-15]. The anode was prepared by subsequently administering TiO_2 paste via the doctor-blade method, using a glass rod and adhesive tape, on the conductive surface of the FTO glass [14-16]. The glass was then annealed at 450 °C for 30 min. The annealed titanium dioxide was immersed in **Rhd** solution overnight. To prepare the cathode, colloidal graphite was applied to the conductive surface of the glass then dried at 150 °C for 15 min [17]. The components of the DSSC device (2cm x 2cm) were assembled by fitting the TiO_2-coated glass on top of the colloidal graphite-coated glass, followed by the introduction of redox iodide/triiodide electrolyte in between them. Rhodamine hydrazide intermediate **1** and target product **Rhd** were synthesized as stated in the literature [9-10] and shown in Scheme 1.

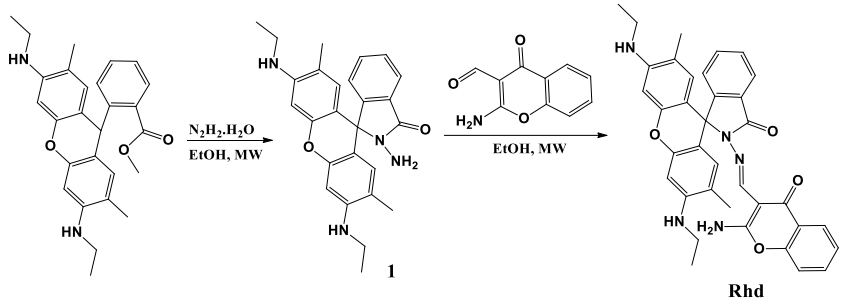

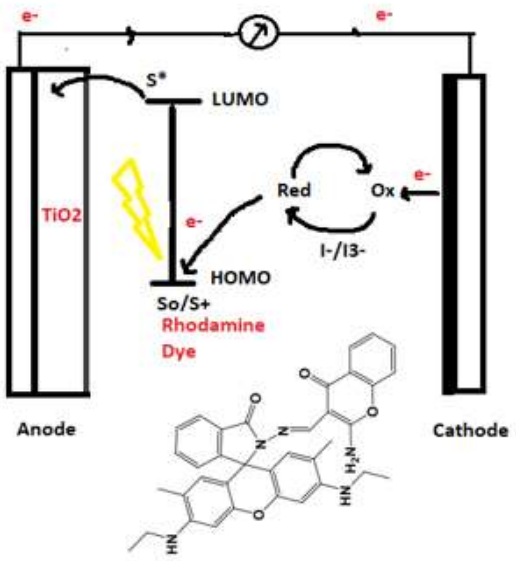

Scheme 1: Microwave assisted synthesis and optical transition using the HOMO-LUMO energy gap.

3. Results and discussion

The sensing ability of **Rhd** was investigated using UV/Vis's absorption and fluorescence spectroscopy. The compound did not show any absorption band above 400 nm, which is typical for the most prominent ring-closed form of rhodamine derivatives [18]. The changes in absorption spectra of **Rhd** with the addition of various metal ions examined in CH_3CN-H_2O (9:1 v/v) tris-HCl system. As shown in Fig.1a, the absorbance of **Rhd** at 530 nm significantly increased in the presence of Al^{3+} with some interference from Cr^{3+} while the absorbance did not show any changes in the presence of other ions. A new absorption band produced at 530 nm demonstrating that a metal-complex was formed, Fig.1b. The sensor **Rhd** exhibited similar fluorescence spectroscopic properties upon binding with Al^{3+} and Cr^{3+} ions, Fig.1c. As shown in Fig.1d, the fluorescence emission for sensor **Rhd** appeared at 560 nm and a significant fluorescence intensity enhancement with 5 equivalents of Al^{3+} ions which indicates **Rhd** is an excellent turn-on sensor for Al^{3+} ions. The detection limits of **Rhd** for Al^{3+} and Cr^{3+} ions were estimated based on the absorbance titration experiment as 42 μM and 37 μM respectively.

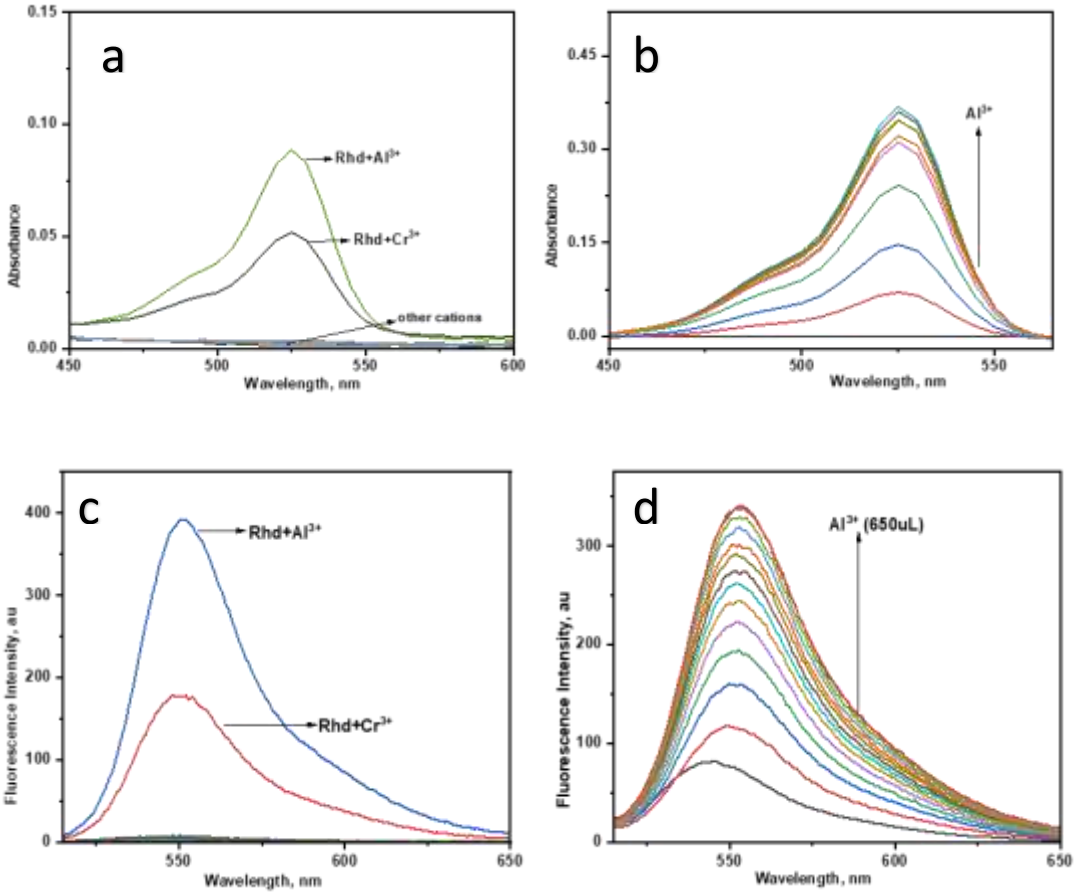

Fig. 1 (**a**) UV/Vis's absorption spectra of **Rhd** with various cations (Co^{2+}, Zn^{2+}, Al^{3+}, Cr^{3+}, Ni^{2+}, Pb^{2+}, Cd^{2+}, Hg^{2+}, Na^{+}, K^{+}, Cu^{2+}, Fe^{2+}, Fe^{3+}, and Ca^{2+}) in CH_3CN/H_2O (9:1 v/v) buffer system (**b**) UV/Vis's absorption spectra of **Rhd** with Al^{3+} (**c**) Fluorescence spectra of **Rhd** with various metal ions (λ_{exc}510 nm), and (**d**) Fluorescence emission spectra of **Rhd** with Al^{3+} ions.

By measuring the current and voltage of the constructed device, it was possible to determine the solar-to-electric power efficiency of the rhodamine DSSCs [19]. The solar-to-electric power conversion efficiency of the rhodamine dye-fabricated device was compared to the efficiencies of rhodamine dye-fabricated devices with aluminum and chromium ions. Fig.2a and Table 1 show the current-density (I-V) characteristics of the dyes under air-mass 1.5 global (AM 1.5 G) illumination having an irradiance of 100 mW/cm^2. An increase in efficiency was observed after the rhodamine dye was made to react with Cr^{3+}, and a decrease in efficiency was observed after the rhodamine dye was made to react with Al^{3+}. The efficiency of the device with **Rhd** alone

was 0.15% but increased to 0.16% after the addition of Cr^{3+}. However, the solar-to-electric power efficiency of the device decreased to 0.14% with the introduction of Al^{3+}. Thus, the introduction of chromium enhanced the light absorption abilities of the rhodamine dye which consequently led to an increase of the efficiencies of the devices fabricated with it.

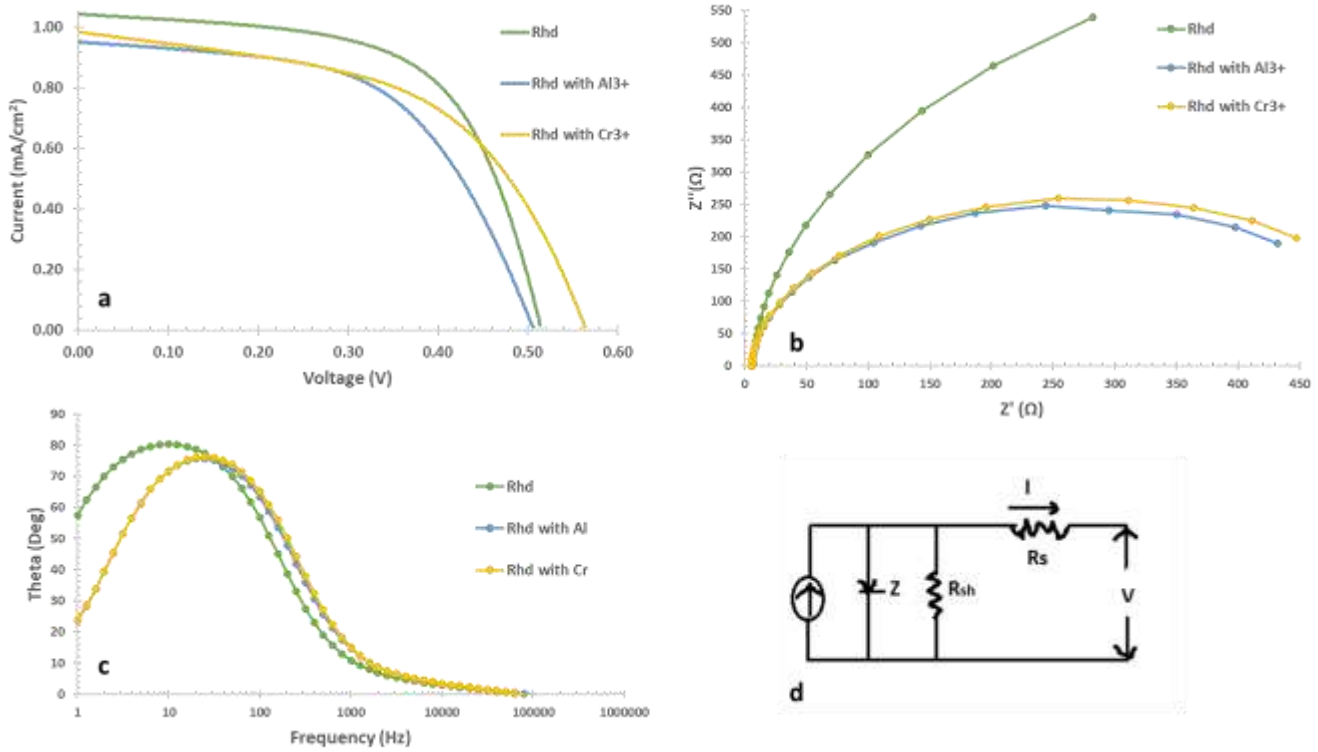

Fig. 2 (a) Current-voltage characteristics, **(b)** Nyquist plot, and **(c)** Bode plot of the rhodamine dye-sensitized solar cell measured under air-mass 1.5 global (AM 1.5 G) illumination having an irradiance of 100 mW/cm^2. (**d**) General representation of equivalent circuits obtained from EIS and I-V characteristics of DSSC.

Table 1. Current and Voltage Measurements for Rhodamine Dye-Sensitized Solar Cells

	V_{max} (V)	I_{max} (mA/cm^2)	V_{oc} (V)	I_{sc} (mA/cm^2)	Fill Factor	Efficiency (%)
Rhd alone	0.37	0.83	0.52	1.04	0.57	0.15
Rhd with Al^{3+}	0.36	0.77	0.51	0.95	0.58	0.14
Rhd with Cr^{3+}	0.42	0.75	0.57	0.99	0.56	0.16

The interfacial charge mechanisms of the DSSCs were addressed using electrochemical impedance spectroscopy (EIS). Impedance measurements are used to investigate the characteristics and quality of DSSCs. They are commonly implemented to investigate the kinetics and energetics of charge recombination and transport in fabricated DSSCs. The Nyquist plot in Fig.2b and Bode plot in Fig.2c show the impedance measurements from the rhodamine devices. Additionally, the Nyquist plot in Fig.2b exhibits well-defined semicircles in the high-frequency regions of the spectra which correspond to the charge-transfer resistance between the counter electrode and redox (I^-/I_3^-) electrolyte. Faster electron transfer rates are associated with smaller resistances, which then result in improved efficiency of the DSSC. Conversely, larger resistances hinder the flow of electrons, thus reducing the performance of the DSSC [20-21]. In the high frequency region of Fig.2b, **Rhd** with Cr^{3+} shows the smallest charge-transfer resistance, and this confirms the current-voltage measurement of **Rhd** with Cr^{3+} having the highest efficiency of 0.16% amongst the other fabricated DSSCs.

From the Bode plots of Fig.2c, the electron lifetimes (τ) of the DSSCs created with **Rhd** alone, **Rhd** with aluminum ion, and **Rhd** with chromium ion were assessed. A higher τ corresponds to a decreased electron recombination rate, and therefore, an increased open circuit voltage V_{oc} [22-23]. Using the formula $\tau = 1/(2\pi f)$, with f being the frequency, the electron lifetime of **Rhd**

alone was calculated to be 16 ms, while **Rhd** with Al^{3+} and **Rhd** with Cr^{3+} having lifetimes of 12 ms. The fabricated DSSC with rhodamine and Al^{3+} having a shorter electron lifetime compared to the DSSC with rhodamine alone agrees with the current-voltage measurements of the V_{oc} of the solar cells. However, **Rhd** with Cr^{3+} having a higher V_{oc} and a shorter electron lifetime than **Rhd** alone is not consistent with the effect of electron recombination rate. This could mean that other factors unrelated to the electron lifetimes affected the value of the V_{oc} for the rhodamine-chromium metal complex.

4. Conclusions

In summary, we have studied a Rhodamine-6G-based dye **Rhd** that operates as a turn-on, fluorescent sensor for Al^{3+} and Cr^{3+} compared to other metal ions. Through current-density characteristics measurements, it was determined that the solar-to-electric power efficiency of solar cells sensitized with **Rhd** and Cr^{3+} (0.16%) was higher than the efficiency of DSSCs with **Rhd** alone (0.15%). EIS measurements of **Rhd** and its metal complexes with Al^{3+} and Cr^{3+} allowed electron lifetime calculations of 16, 12, and 12 ms, respectively. These impedance measurements also displayed that the solar cells sensitized with **Rhd** and Cr^{3+} ion had the smallest charge transfer resistance, leading to a higher efficiency of the DSSC.

Declaration of Competing Interest

The authors declare that they have no known competing financial interests or personal relationships that could have appeared to influence the work reported in this paper.

Data availability

Data will be made available on request

Acknowledgments

This research was funded by the National Science Foundation's Division of Chemistry under grant [2100629] and National Institute of General Medical Sciences under [SC2GM125512] grants awarded to Morgan State University.

References

1) G.K. Singh, Energy 53 (2013) 1–13.
2) G.D.A. Jebaselvi, et al., Renew. Sust. Energ. Rev. 28 (2013) 625–634.
3) J. Baldenebro-López, et al., J. Photochem. Photobiol. A 267 (2013) 1–5.
4) B. O'Regan, et al., Nature 353 (1991) 737-740.
5) F. Bella, et al., Chem. Soc. Rev. 44(11) (2015) 3431–3473.
6) F. Abebe, et al., ACS Omega 7(17) (2022) 14611–14621.
7) M.D. Tyona., et al., Mater. Lett. 220 (2018) 281–284.
8) F. Abebe, et al., J. Mol. Struct. 1205 (2020) 127594.
9) B. Ranamagar, et al., Green Sustain. Chem. 12(3) (2022) 57–72.
10) F. Abebe, et al., Luminescence 33(7) (2018) 1194–1201.
11) S. Chemate, et al., Sens. Actuators B Chem. 220 (2015) 1196–1204.
12) E.B. Lindblad, Immunol. Cell Biol. 82(5) (2004) 497–505.
13) J. Salimian, et al., J. Mater. Res. Technol. 18 (2022) 4816–4833.
14) A. Mashreghi, et al., Mater. Sci. Semicond. 30 (2015) 618–624.
15) T. N. Thanh, et al., ACS Appl. Mater. Interfaces 13 (2021) 10181-101190.
16) K. Gossen, et al., Optik 183 (2019) 253–256.
17) I.J. Junger, et al., Optik 174 (2018) 40–45.
18) H. He, et al., Molecules 26(2) (2021) 512.
19) D. Kabir, et al., Nano-Struct. Nano-Objects 26 (2021) 100698.
20) F. Saadmim, et al., Molecules 25(17) (2020) 4021.
21) P. Malkeshkumar, et al., ACS Appl. Mater. Interfaces 6 (2014) 10099-10106.
22) G. Pacchioni, ChemPhysChem 4 (2003) 1041−1047.
23) B.J. Morgan, et al., J. Phys. Chem. C 116 (2012) 7242.